Datasheet for 600-401-215

GFP Antibody

Overview

Description:	Anti-GFP (RABBIT) Antibody - 600-401-215
Item No.:	600-401-215
Size:	100 µg
Applications:	ELISA, WB, CUT&RUN, EM, FC, IF, IHC, IP, Microarray, Multiplex, Other, Purification
Reactivity:	GFP, eGFP, rGFP, RS-GFP, S65T-GFP, YFP
Host Species:	Rabbit

Product Details

Background:	Green Fluorescent Protein (GFP) is a 27 kDa protein produced from the jellyfish Aequorea victoria, which emits green light (emission peak at a wavelength of 509nm) when excited by blue light. GFP is an important tool in cell biology research. GFP is widely used enabling researchers to visualize and localize GFP-tagged proteins within living cells without the need for chemical staining. GFP Antibody is ideal for Cell Biology, Neuroscience and Cancer research.
Synonyms:	rabbit anti-GFP antibody, Green Fluorescent Protein, GFP antibody, Green Fluorescent Protein antibody, EGFP, enhanced Green Fluorescent Protein, Aequorea victoria, Jellyfish
Host Species:	Rabbit
Clonality:	Polyclonal
Format:	IgG

Target Details

Reactivity:	GFP, eGFP, rGFP, RS-GFP, S65T-GFP, YFP
Immunogen Type:	Recombinant Protein
Immunogen:	The immunogen is a Green Fluorescent Protein (GFP) fusion protein corresponding to the full length amino acid sequence (246aa) derived from the jellyfish Aequorea victoria.

Purity/Specificity:	Anti-GFP antibody was prepared from monospecific antiserum by immunoaffinity chromatography using Green Fluorescent Protein (Aequorea victoria) coupled to agarose beads followed by solid phase adsorption(s) to remove any unwanted reactivities. Assay by immunoelectrophoresis resulted in a single precipitin arc against anti-Rabbit Serum and purified and partially purified Green Fluorescent Protein (Aequorea victoria). No reaction was observed against Human, Mouse or Rat serum proteins.
Relevant Links:	• 600-401-215 SDS • UniProtKB - P42212

Application Details

Tested Applications:	ELISA, WB
Suggested Applications:	CUT&RUN, EM, FC, IF, IHC, IP, Microarray, Multiplex, Other, Purification (Based on references)
Application Note:	Anti-GFP antibody is designed to detect GFP and its variants. GFP antibody has been tested by western blot and ELISA. This product can be used to detect GFP by ELISA (sandwich or capture) for the direct binding of antigen and recognizes wild type, recombinant and enhanced forms of GFP. Biotin conjugated polyclonal anti-GFP used in a sandwich ELISA is well suited to titrate GFP in solution using this antibody in combination with Rockland's monoclonal anti-GFP (600-301-215) using either form of the antibody as the capture or detection antibodies. However, use the monoclonal form only for the detection of wild type or recombinant GFP as this form does not sufficiently detect 'enhanced' GFP. The detection antibody is typically conjugated to biotin and subsequently reacted with streptavidin conjugated HRP (code # S000-03). Fluorochrome conjugated polyclonal anti-GFP can be used to detect GFP by immunofluorescence microscopy in prokaryotic (E.coli) and eukaryotic (CHO cells) expression systems and can detect GFP containing inserts. Significant amplification of signal is achieved using fluorochrome conjugated polyclonal anti-GFP relative to the fluorescence of GFP alone. For immunoblotting use either alkaline phosphatase or peroxidase conjugated polyclonal anti-GFP to detect GFP or GFP containing proteins on western blots. Optimal titers for applications should be determined by the researcher.
Assay Dilutions:	All assays should be optimized by the user. Recommended dilutions (if any) may be listed below.
ELISA:	1:20,000 - 1:120,000
FC:	User Optimized
IF:	1:500 - 1:5,000
IHC:	1:200 - 1:3,000
IP:	User Optimized
WB:	1:500 - 1:5,000
Other:	Immuno-EM, TEM

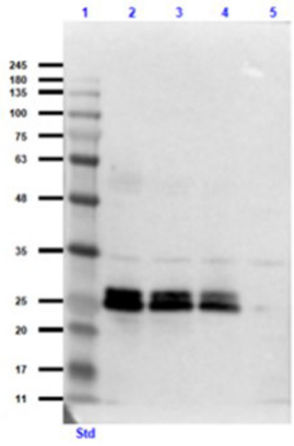
Formulation

Physical State:	Liquid (sterile filtered)
Concentration:	1.25 mg/mL by UV absorbance at 280 nm
Buffer:	0.02 M Potassium Phosphate, 0.15 M Sodium Chloride, pH 7.2
Preservative:	0.01% (w/v) Sodium Azide
Stabilizer:	None

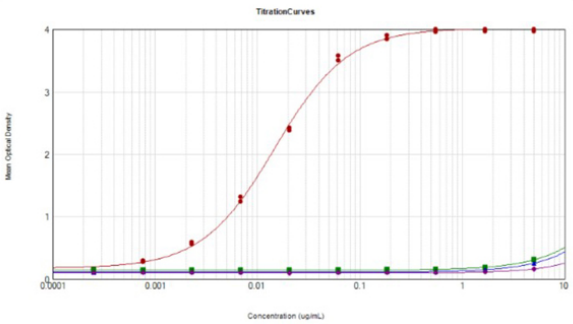
Shipping & Handling

Shipping Condition:	Dry Ice
Storage Condition:	Store Anti-GFP Antibody at -20° C prior to opening. Aliquot contents and freeze at -20° C or below for extended storage. Avoid cycles of freezing and thawing. Centrifuge product if not completely clear after standing at room temperature. GFP antibody is stable for several weeks at 4° C as an undiluted liquid. Dilute only prior to immediate use.
Expiration:	Expiration date is one (1) year from date of receipt.

Images

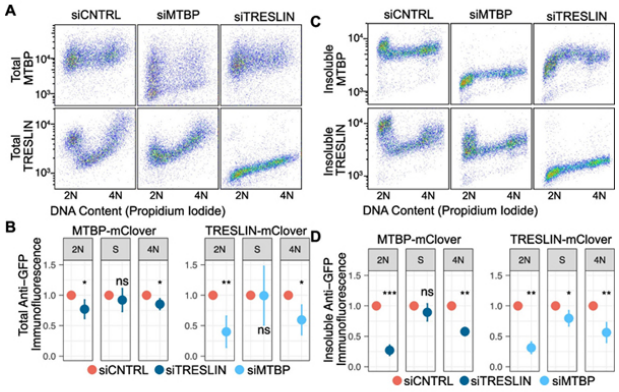


Western Blot
Western Blot of Rabbit Anti-GFP Antibody.
Lane 1: Opal Prestained Molecular Weight Ladder (p/n MB-210-0500).
Lane 2: GFP (p/n 000-001-215) / HeLa Lysate (p/n W09-000-364) [0.1µg/10.0µg].
Lane 3: GFP (p/n 000-001-215) / HeLa Lysate (p/n W09-000-364) [0.05µg/10.0µg].
Lane 4: GFP (p/n 000-001-215) / HeLa Lysate (p/n W09-000-364) [0.03µg/10.0µg].
Lane 5: HeLa Lysate (p/n W09-000-364) [10.0µg].
Primary Antibody: Rabbit Anti-GFP Antibody at 1.0µg/mL overnight at 2-8°C.
Secondary Antibody: Goat Anti-Rabbit IgG MX 10 Peroxidase (p/n 611-103-122) at 1:70,000 for 30mins at RT.
Block: Blocking Buffer for Fluorescent Western Blotting (p/n MB-070) for 60 mins at RT.
Expect: ~27kDa.



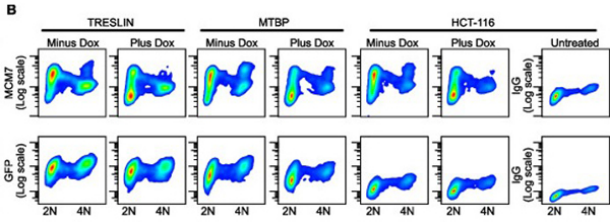
ELISA

ELISA results of purified Rabbit Anti-GFP Antibody. Each well was coated in 10 µg of antigen GFP [Red Line], human IgG [Green Line], Mouse IgG [Blue Line], and Rat IgG [Purple Line]. The starting dilution of antibody was 5 µg/mL and the X-axis represents the Log10 of a 3-fold dilution. The titer is 1:67,700. This titration is a 4-parameter curve fit where the IC50 is defined as the titer of the antibody. Assay performed using 1% Fish Gel, TMB Substrate (p/n TMB-1000), and Goat Anti-Rabbit IgG Antibody HRP (p/n 611-103-122).



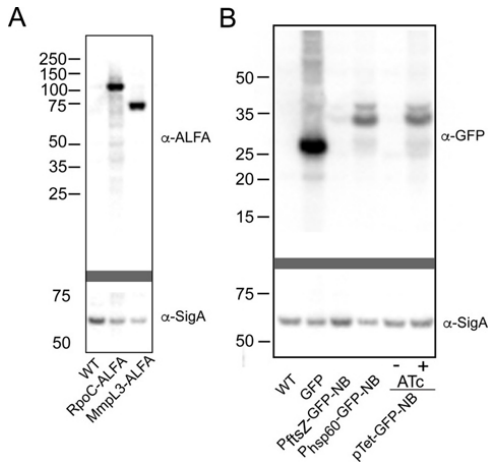
Flow Cytometry

Binding of MTBP to chromatin requires TRESLIN in G1 but not in S. A Protein levels of MTBP-mClover and TRESLIN-mClover in HCT116 cells were measured via flow cytometry using an anti-GFP antibody, alongside DNA content. This analysis was conducted 24 h after siRNA transfection, representing a single experimental replicate. B Quantification of the data in panel A involved background-subtracting individual cell anti-GFP immunofluorescence signals, averaging signals for cells in 2 N, early S, or 4 N DNA content gates, and normalizing values from siTRESLIN or siMTBP transfected cells to siCNTRL. The means of these normalized values across three replicates are shown with error bars indicating 95% confidence intervals. Asterisks indicate significance levels from t-tests comparing each sample to its respective siCNTRL. C–D replicate (A) and (B), respectively, with the exception that soluble protein was pre-extracted before fixation. Consequently, immunofluorescence signals represent insoluble TRESLIN-mClover or MTBP-mClover protein. Fig 4. PMID: 40624716



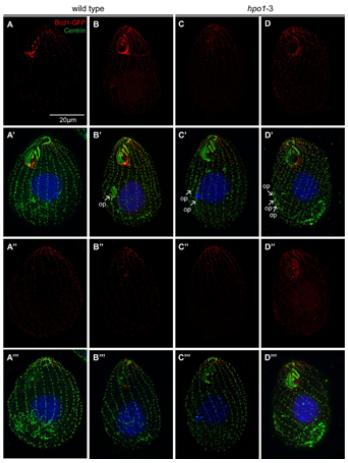
Flow Cytometry

B Insoluble flow cytometry showing level of chromatin bound MCM7 and TRESLIN-mClover or MTBP-mClover in tagged (TRESLIN or MTBP) or untagged (HCT-116) cells. Anti-MCM7, anti-GFP, or anti-IgG immunofluorescence signal vs DNA content is plotted to show the level of each protein across the cell cycle. Treatment with doxycycline for 16 h was sufficient to reduce levels of chromatin bound MCM7 in 2 N cells. TRESLIN binding was unaffected while MTBP binding was partially reduced. Fig 5. PMID: 40624716



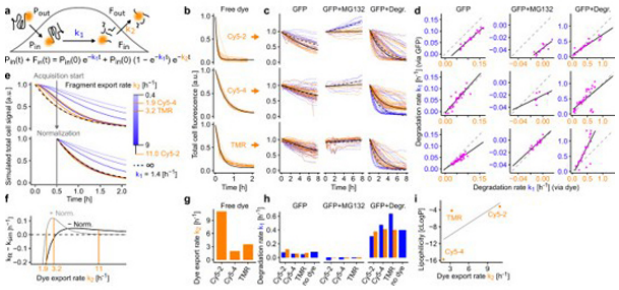
Western Blot

Chromosomal ALFA-tagged MmpL3 and RpoC. (A) Immunoblots of lysates from MC2155 (WT), MGM7103 (encoding RpoC-ALFA), and MGM7059 (encoding MmpL3-ALFA). The top blot is probed using NBALFA and anti-VHH-HRP. The bottom blot is stripped and probed with anti-SigA and anti-rabbit Ig-horseradish peroxidase (HRP) as a loading control. (B) Immunoblots of lysates from MC2155, MGM6970 (expressing GFP), MGM7087 (expressing GFP-NBALFA from the PftsZ1 promoter), MGM7089 (expressing GFP-NBALFA from the Phsp60 promoter), MGM7047 (expressing TetON GFP-NBALFA, no ATc), and MGM7047 (encoding TetON GFP-NBALFA, +ATc-50 ng/mL). Top blot probed with anti-GFP and anti-rabbit Ig-HRP. Bottom blot stripped and probed with anti-SigA and anti-rabbit Ig-HRP. Fig 2. PMID: 40576343



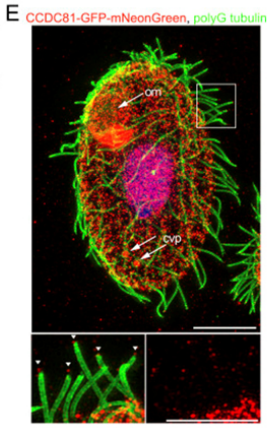
Immunofluorescence Microscopy

(A-D”’) Pairs of SR-SIM images showing two sides of the same cells that express Bcd1-GFP and are either otherwise wild-type (A-B”’) or hpo1-3 (C-D”’). The cells were labeled with the anti-GFP antibodies (red), 20H5 anti-centrin antibody (green), and DAPI (blue) after a period of growth for 4 hours at 39°C. SF5. PMID: 40455876

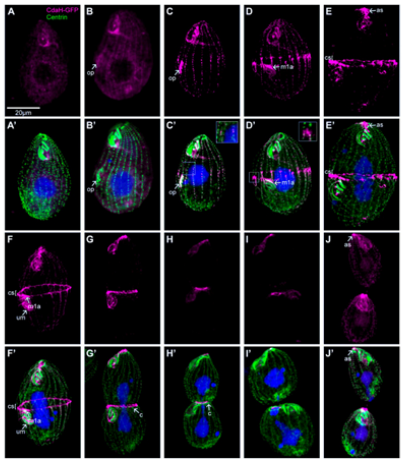


Immunofluorescence Microscopy

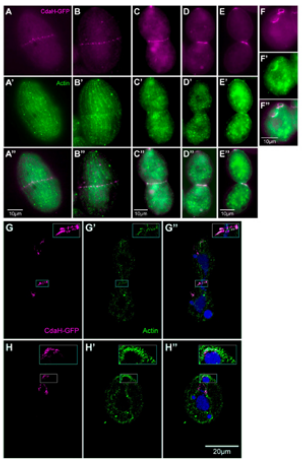
Site-specific coupling to small-molecule chromophores as reporters for protein degradation. (a) A model describing total cell fluorescence (TCF) changes as a result of protein degradation and subsequent cellular export of fragments. P refers to the labeled protein, F to the labeled degradation fragments, k1 to the degradation rate constant and k2 to the overall export rate constant. (b) TCF of single cells upon microinjection of dyes containing a maleimide group, quenched before injection with excess β-mercaptoethanol. The black line indicates the averaged degradation rate from an exponential decay model with a non-zero plateau parameter. (c) eGFP degradation was followed simultaneously by its intrinsic fluorescence and by an attached dye (indicated next to the orange arrow). eGFP fluorescence as a function of time is shown with dashed blue lines, while solid orange lines indicate dye signal. Black lines indicate simulated signal changes for a cell with averaged degradation rate (dashed, eGFP fluorescence; solid, respective dye fluorescence). The simple exponential decay model was used, except for eGFP coupled to Cy5-4 and co-injected with a bioPROTAC (see main text), where a free plateau parameter was introduced for fitting. Top row, Cy5-2; middle row, Cy5-4; bottom row, TMR. (d) Correlation between the degradation rate determined by loss of GFP fluorescence and from loss of fluorescence of small-molecule dyes attached to GFP. A perfect correlation would be indicated by the dashed grey line going through zero, while the linear regression line is shown in black. Top row, Cy5-2; middle row, Cy5-4; bottom row, TMR. (e) Simulated TCF data assuming a fixed degradation rate constant of a protein with a 30 min half-life and a range of dye export rates. Top, actual kinetics; bottom, apparent kinetics, if the observed traces are normalized at the first measured point after 0.5 h. (f) The difference between true and fitted simulated data using a first order exponential decay model is plotted against the dye export rates. The result of fitting with the exclusion of the first 30 min after injection is indicated in black, whereas fitting of data from the injection start is shown in grey. (g) Measured dye export rates. (h) Bar heights indicate averaged degradation rate constants based on eGFP (blue, left bar) or dye signal (orange, right bar); “Degr.” denotes bioPROTAC (see main text). (i) Calculated partition coefficient (cLogP) versus observed dye export rate. Fig 4.
PMID: 39511251



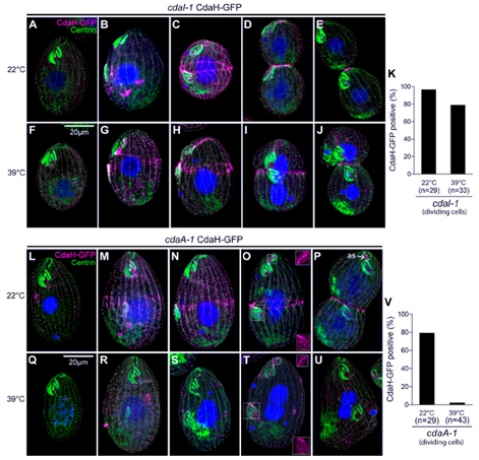
Immunofluorescence Microscopy
(E) Representative SR-SIM images of cells expressing CCDC81-GFP-mNeonGreen under the native promoter fixed and labeled with AXO49 anti-polyglycylated (polyG) tubulin monoclonal antibody that labels ciliary axonemes (green), anti-GFP polyclonal antibodies (red), and DAPI (blue). Inset highlights CCDC81 at the tips of locomotory lateral cilia. Scale bars 10 µm, inset 5 µm. Abbreviations: om, oral membranelle; cvp, contractile vacuole pore. Arrowheads point to ciliary tips. Fig 6. PMID: 37756660



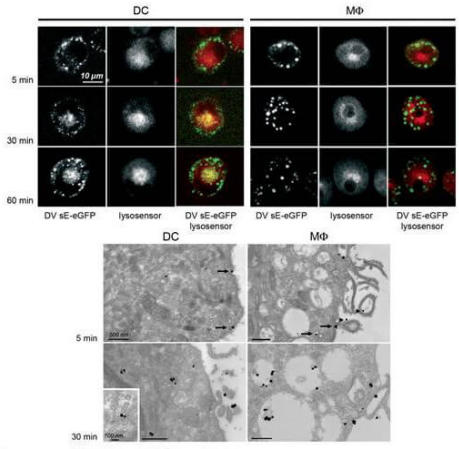
Immunofluorescence Microscopy
CdaH–GFP accumulates at multiple locations during cell division. Confocal images of cells expressing CdaH–GFP, arranged according to the cell cycle stage. The cells were labeled by anti-GFP (magenta) and anti-centrin (green) antibodies and DAPI (blue). (A,A') Interphase. Note that antibodies frequently bind to the OA, especially its posterior region, resulting in background fluorescence (Jiang et al., 2017). (B–C') Early OP development. (D,D') Onset of cortical subdivision. The OP is in an advanced stage, and all rows are visible. (E–H') Cytokinesis and formation of new cell ends. (I–J') Scission. The images are representative of five independent immunofluorescence experiments. as, anterior suture; c, BB couplet; cs, cortical subdivision; m1a, M1 arc; op, oral primordium; um, undulating membrane. Scale bar: 20 µm. Fig 4.
PMID: 37667859



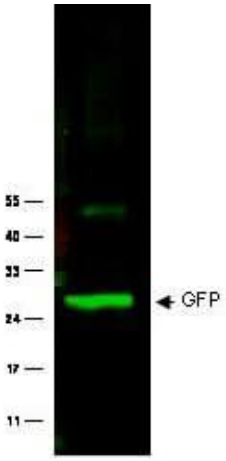
Immunofluorescence Microscopy
CdaH–GFP colocalizes with actin at the anterior margin of the posterior daughter cell. (A–F″) The CdaH–GFP-expressing cells were fixed with cold methanol and labeled with polyclonal anti-Act1 actin antibodies (green) and CdaH–GFP was imaged directly (magenta). (A–A″) Cortical subdivision prior to cytokinesis. (B–E″) Stages of cytokinesis. (F–F″) An early posterior post-divider. The images shown in panels A–F″ are representative of four independent experiments. (G–H″) SR-SIM images of cells fixed with paraformaldehyde in a late stage of cytokinesis around at the time of scission (G–G″) and of a posterior post-divider shortly after scission (H–H″) labeled with anti-GFP (magenta), anti-Act1 (green) and DAPI (blue). Note that, using this fixation method, the direct GFP signal of CdaH–GFP was not visible in the green channel. The images shown in panels G–H″ are representative of two independent experiments. Scale bars: 10 μm (A–F″); 20 μm (G–H″). Fig 6.
PMID: 37667859



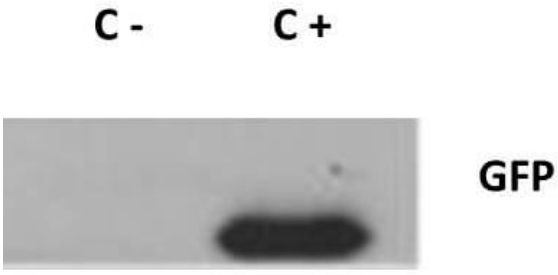
Immunofluorescence Microscopy
CdaA, but not CdaI, is required for proper distribution of CdaH. (A–J) Confocal images of cdaI-1 cells expressing CdaH–GFP, labeled with anti-GFP (magenta), anti-centrin (green) and DAPI (blue). Prior to staining, cells were incubated at either 22°C (A–E) or 39°C (F–J) for 2 h. (K) The graph shows the percentage of dividing cells with a (stage-appropriate) pattern of CdaH–GFP. (L–U) Confocal images of cdaA-1 cells expressing CdaH–GFP, labeled with anti-GFP (magenta), anti-centrin (green) and DAPI (blue), incubated at either 22°C (L–P) or 39°C (Q–U) for 2 h. (V) The graph shows the percentage of dividing cells with CdaH–GFP in the form of either posterior streaks or a subequatorial ring (sub-pools associated with the cortical subdivision and cytokinesis). The images shown are representative of three independent experiments. Scale bars: 20 μm. Fig 7. PMID: 37667859



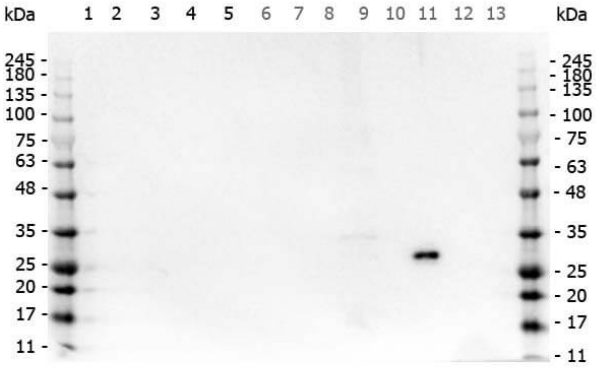
Immunofluorescence Microscopy
Immuno-microscopy of Rabbit anti-GFP antibody. Monocyte derived dendritic cells and dermal macrophages were challenged and directly visualized with eGFP labeled Dengue virus to localize sequestration of virus particles in the different cells (upper). The location of the GFP was confirmed by TEM (lower magnified view) using Rockland rabbit anti GFP Primary antibody (1:200) and a gold labeled secondary antibody. As referenced in: Kwan W-H, Navarro-Sanchez E, Dumortier H, Decossas M, Vachon H, et al. (2008) Dermal-Type Macrophages Expressing CD209/DC-SIGN Show Inherent Resistance to Dengue Virus Growth. PLoS Negl Trop Dis 2(10): e311. doi:10.1371/journal.pntd.0000311



Western Blot
Western Blot of Rabbit anti-GFP antibody. Lane 1: Wild type GFP (0.1 µg) was used to spike HeLa whole cell lysate. Lane 2: none. Load: 30 µg per lane. Primary antibody: GFP antibody at 1:1000 for overnight at 4°C. Secondary antibody: IRDye800™ Goat-a-Rabbit IgG [H&L] MX10 (611-132-122) at 1:10,000 for 45 min at RT. Block: 5% BLOTTO in PBS overnight at 4°C. Predicted/Observed size: 27 kDa for epitope tag GFP. Other band(s): none.



Western Blot
Western Blot of Rabbit anti-GFP antibody. Lane 1: 293FT cells transfected with CDK4 dominant negative (C-). Lane 2: 293FT cells poitive control (C+). Load: 25 µg per lane. Primary antibody: GFP antibody at 1:400 for overnight at 4°C. Secondary antibody: IRDye800™ rabbit secondary antibody at 1:10,000 for 45 min at RT. Block: 5% BLOTTO overnight at 4°C. Predicted/Observed size: 27 kDa for GFP.



Western Blot

Western Blot of Rabbit anti-GFP antibody. Marker: Opal Pre-stained ladder (p/n MB-210-0500). Lane 1: HEK293 lysate (p/n W09-000-365). Lane 2: HeLa Lysate (p/n W09-000-364). Lane 3: CHO/K1 Lysate (p/n W07-000-357). Lane 4: MDA-MB-231 (p/n W09-001-GK6). Lane 5: A431 Lysate (p/n W09-000-361). Lane 6: Jurkat Lysate (p/n W09-001-370). Lane 7: NIH/3T3 Lysate (p/n W10-000-358). Lane 8: E-coli HCP Control (p/n 000-001-J08). Lane 9: FLAG Positive Control Lysate (p/n W00-001-383). Lane 10: Red Fluorescent Protein (p/n 000-001-379). Lane 11: Green Fluorescent Protein (p/n 000-001-215). Lane 12: Glutathione-S-Transferase Protein (p/n 000-001-200). Lane 13: Maltose Binding Protein (p/n 000-001-385). Load: 10 µg of lysate or 50ng of purified protein per lane. Primary antibody: GFP antibody at 1ug/mL overnight at 4C. Secondary antibody: Peroxidase rabbit secondary antibody (p/n 611-103-122) at 1:30,000 for 60 min at RT. Blocking Buffer: 1% Casein-TTBS (p/n MB-082) for 30 min at RT. Predicted/Observed size: 30 kDa for GFP.

References

- Jiang M et al. Butyrate causes loss of specific acetylation by the histone acetyltransferase p300. *iScience.* (2026)
- Cole ES et al. Tetrahymena JanusA gene encodes a polo kinase whose loss triggers a dorsal/ventral intracellular homeosis. *Curr Biol.* (2026)
- Leonard SP et al. Synthetic overlapping genes stabilize genetic systems. *mBio.* (2026)
- Bian J et al. PVNCRF Neurons Regulate Migraine-Like Allodynia by Activating CRFR2 on Spinal Trigeminal Caudalis Glutamatergic Neurons. *Adv Sci (Weinh).* (2026)
- Shah SS et al. NEDD4L-mediated Gasdermin D and E ubiquitination regulates cell death and tissue injury. *Cell Death Differ.* (2026)
- Fink S et al. Glomerulus-Specific Inhomogeneity of the Basal Activity Map in the Olfactory Bulb. *Int J Mol Sci.* (2026)
- Zhao J et al. Cell-type-specific autophagy in root-hair-forming cells is essential for salt stress tolerance in Arabidopsis thaliana. *Nat Plants.* (2026)
- Rühl S et al. Inhibition of BAK-mediated apoptosis by the BH3-only protein BNIP5. *Cell Death Differ.* (2025)
- Duke LC et al. Tetraspanin CD9 alters cellular trafficking and endocytosis of tetraspanin CD63, affecting CD63 packaging into small extracellular vesicles. *J Biol Chem.* (2025)
- Châtel-Soulet HÉ et al. Thrombopoietin increases susceptibility for EVI1 + KMT2A-MLLT3-driven AML expressing stem cell genes linked to poor outcome. *Nat Commun.* (2025)

- Willoughby JJ et al. Abca4, mutated in Stargardt disease, is required for structural integrity of cone outer segments. *Dis Model Mech.* (2025)
- Hwang J et al. Liver-innervating vagal sensory neurons are indispensable for the development of hepatic steatosis and anxiety-like behavior in diet-induced obese mice. *Nat Commun.* (2025)
- Ferns M et al. The Electrically Silent Kv5.1 Subunit Forms Heteromeric Kv2 Channels in Cortical Neurons and Confers Distinct Functional Properties. *J Neurosci.* (2025)
- Pissarek H et al. Formin 3 stabilizes the cytoskeleton of Drosophila tendon cells, thus enabling them to resist muscle tensile forces. *J Cell Sci.* (2025)
- Deraniyagala AS et al. Importin-9 and a TPR domain protein MpH drive periodic patterning of ciliary arrays in Tetrahymena. *J Cell Biol.* (2025)
- Cheng AP et al. Fungal Argonaute proteins act in bidirectional cross-kingdom RNA interference during plant infection. *Proc Natl Acad Sci U S A.* (2025)
- Konate K et al. WRAP-based nanoparticles for siRNA delivery in zebrafish embryos by simple bath immersion. *Mol Ther Methods Clin Dev.* (2025)
- Kemp Jr JP et al. Cell-cycle-regulated transcriptional pausing of Drosophila replication-dependent histone genes. *Mol Biol Cell.* (2025)
- Hasselmann T, et al. The PDE4D ortholog Dunce suppresses memory in Drosophila melanogaster. *BioRxiv (Preprint)* (2025)
- Teko-Agbo cA et al. A short peptide for efficient cellular mRNA delivery: A potential application for inducing an immune response. *Mol Ther Nucleic Acids.* (2025)
- Boada-Romero et al. Membrane receptors cluster phosphatidylserine to activate LC3-associated phagocytosis. *Nat Cell Biol.* (2025)
- Kolibius J et al. Genome-replicating HC-AdV: A novel high-capacity adenoviral vector class featuring enhanced in situ payload expression. *Mol Ther Methods Clin Dev.* (2025)
- Green WD et al. Enhancer-driven gene regulatory networks reveal transcription factors governing T cell adaptation and differentiation in the tumor microenvironment. *Immunity.* (2025)
- Legal T et al. Structure of the ciliary tip central pair reveals the unique role of the microtubule-seam binding protein SPEF1. *Curr Biol.* (2025)
- Kang W et al. Time-dependent catalytic activity in aging condensates. *Nat Commun.* (2025)
- Yuem ELH et al. Membrane contact sites between chloroplasts and the pathogen interface underpin plant focal immune responses. *Plant Cell.* (2025)
- Lacey TA et al. Kv2/Kv6.4 Heteromeric Potassium Channels Are Expressed in Spinal Motoneurons and Localized at C-Bouton Synapses. *Eur J Neurosci.* (2025)
- Chen T et al. Phosphorylation of VAMP3 couples IL-6 exocytosis to dendritic cell activation. *J Cell Sci.* (2025)
- Nishat K et al. IFT139 regulates Hedgehog signaling and cilia structure through ciliary protein localization. *Biol Open.* (2025)

- Gillespie WB 3rd et al. MultiSite Assembly of Gateway Induced Clones (MAGIC): a flexible cloning toolbox for use in vertebrate model systems. *Development.* (2025)
- Fay A et al. A split ALFA tag-nanobody system for protein localization and proximity proteomics in mycobacteria. *mBio.* (2025)
- Lee C et al. Left-right cortical interactions drive intracellular pattern formation in the ciliate Tetrahymena. *PLoS Genet.* (2025)
- Winkelvoß D et al. Molecular features defining the efficiency of bioPROTACs. *Commun Biol.* (2025)
- Noble TD et al. Cell Cycle-Dependent TICRR/TRESLIN and MTBP Chromatin Binding Mechanisms and Patterns. *Genome Biol.* (2024)
- Kirk AM et al. DNAJB1-PRKACA fusion neoantigens elicit rare endogenous T cell responses that potentiate cell therapy for fibrolamellar carcinoma. *Cell Rep Med.* (2024)
- Vukovic D et al. Protein degradation kinetics measured by microinjection and live-cell fluorescence microscopy. *Sci Rep.* (2024)
- Lee C et al. Global and local functions of the Fused kinase ortholog CdaH in intracellular patterning in Tetrahymena. *J Cell Sci.* (2024)
- Zhang W et al. A Bioresponsive Genetically Encoded Antimicrobial Crystal for the Oral Treatment of Helicobacter Pylori Infection. *Adv Sci (Weinh).* (2023)
- Walton K et al. Site-specific phosphorylations of the Arf activator GBF1 differentially regulate GBF1 function in Golgi homeostasis and secretion versus cytokinesis. *Sci Rep.* (2023)
- Chaubal A et al. Coordinated expression of replication-dependent histone genes from multiple loci promotes histone homeostasis in Drosophila. *Mol Biol Cell.* (2023)
- Martinez AP et al. Pcdh19 mediates olfactory sensory neuron coalescence during postnatal stages and regeneration. *iScience.* (2023)
- Müller L et al. Plakophilin 3 facilitates G1/S phase transition and enhances proliferation by capturing RB protein in the cytoplasm and promoting EGFR signaling. *Cell Rep.* (2023)
- Navyasree KV et al. Cholesterol regulates insulin-induced mTORC1 signaling. *J Cell Sci.* (2023)
- Sun Y et al. Focal-adhesion kinase regulates the sialylation of N-glycans via the PI4KIIα-PI4P pathway. *J Biol Chem.* (2023)
- Legal T et al. CEP104/FAP256 and associated cap complex maintain stability of the ciliary tip. *J Cell Biol.* (2023)
- Frasch M et al. The RNF220 domain nuclear factor Teyrha-Meyrha (Tey) regulates the migration and differentiation of specific visceral and somatic muscles in Drosophila. *Development.* (2023)
- Müller L et al. Protocol to determine the subcellular localization of protein interactions in murine keratinocytes. *STAR Protoc.* (2023)
- Kimoto A et al. Exosomes in ascites from patients with human pancreatic cancer enhance remote metastasis partially through endothelial-mesenchymal transition. *Pancreatology.* (2023)
- Yang HJ et al. A nuclear pore complex-associated regulation of SUMOylation in meiosis *Genes Cells.* (2023)
- View More ...

www.rockland.com
tech@rockland.com
+1 484.791.3823

Disclaimer

This product is for research use only and is not intended for therapeutic or diagnostic applications. Please contact a technical service representative for more information. All products of animal origin manufactured by Rockland Immunochemicals are derived from starting materials of North American origin. Collection was performed in United States Department of Agriculture (USDA) inspected facilities and all materials have been inspected and certified to be free of disease and suitable for exportation. All properties listed are typical characteristics and are not specifications. All suggestions and data are offered in good faith but without guarantee as conditions and methods of use of our products are beyond our control. All claims must be made within 30 days following the date of delivery. The prospective user must determine the suitability of our materials before adopting them on a commercial scale. Suggested uses of our products are not recommendations to use our products in violation of any patent or as a license under any patent of Rockland Immunochemicals, Inc. If you require a commercial license to use this material and do not have one, then return this material, unopened to: Rockland Inc., P.O. BOX 5199, Limerick, Pennsylvania, USA.